COMPUTER-AIDED DESIGN & APPLICATIONS, 2018
VOL. 15, NO. 1, 25–33
https://doi.org/10.1080/16864360.2017.1353727

Taylor & Francis
Taylor & Francis Group

Check for updates

A novel hierarchical clustering algorithm for the analysis of 3D anthropometric data of the human head

Thierry Ellena [a], Aleksandar Subic [b], Helmy Mustafa [a] and Toh Yen Pang [a]

[a] School of Engineering, RMIT University, Australia; [b] Swinburne University of Technology, Australia

ABSTRACT

In recent years, the use of 3D anthropometry for product design has become more appealing because of advances in mesh parameterisation, multivariate analyses and clustering algorithms. The purpose of this study was to introduce a new method for the clustering of 3D head scans. A novel hierarchical algorithm was developed, in which a squared Euclidean metric was used to assess the head shape similarity of participants. A linkage criterion based on the centroid distance was implemented, while clusters were created one after another in an enhanced manner. As a result, 95.0% of the studied sample was classified inside one of the four computed clusters. Compared to conventional hierarchical techniques, our method could classify a higher ratio of individuals into a smaller number of clusters, while still satisfying the same variation requirements within each cluster. The proposed method can provide meaningful information about the head shape variation within a population, and should encourage ergonomists to use 3D anthropometric data during the design process of head and facial gear.

KEYWORDS

3D anthropometric data; clustering algorithm; hierarchical algorithm

1. Introduction

One of the main objectives of human factors, when applied to engineering and industrial design, is to conceive equipment and devices that closely "fit" the people who use them. This is usually accomplished by collecting and processing anthropometric data of a group of users, describing the body dimensions relevant for the specific design. Subsequently, these data need to be summarised in a simplified and useful manner in order to be used efficiently by the product design team.

The recent developments in 3D scanning technologies have encouraged the use of 3D anthropometric measurements for product design [6,22,24,25]. These data provide an in-depth description of the size and shape characteristics of the scanned subjects due to the large set of data points they contain. However, it remains difficult to analyse proficiently these data and to present body shape information in a summarised form for the population of interest. As the type of information provided to designers must be simplified, size and shape characteristics are typically presented as a series of generic models; i.e., mannequins and headforms. To create these models, it is necessary to first group subjects with similar size and shape attributes into a set of representative clusters. Multiple methods have been presented in the past to describe how these groups could be created. However, only a few focused on 3D data only. In this study, we introduce an original method based on clustering algorithms.

Arguably, the following requirements should be satisfied when creating clusters of individuals for 3D-sizing systems;

- first, the generated clusters should be as compact as possible to favour better-fitted designs of ergonomic products such as helmets (for 3D head scans, the whole geometry of the head should be similarly shaped for all subjects in a cluster),
- second, the method should be robust against outliers to avoid the creation of too many clusters (very dissimilar objects could belong to no clusters), but should also aim to accommodate a large ratio of people from the studied population,
- third, the method should be able to capture clusters with various densities and shapes in order to represent the full spectrum of the 3D shapes considered. Indeed, while it is envisaged that a large proportion of the data could be clustered in a couple of very dense clusters, it

CONTACT Thierry Ellena t.perretellena@gmail.com; Aleksandar Subic asubic@swin.edu.au; Helmy Mustafa helmy.mustafaelbakri@rmit.edu.au; Toh Yen Pang tohyen.pang@rmit.edu.au

[This article was originally published with errors. These have now been corrected. Please see Corrigendum: https://doi.org/10.1080/16864360.2017.1359906]

© 2017 CAD Solutions, LLC, http://www.cadanda.com

is important that less frequent shapes are also detected,
- fourth, the algorithm's complexity should be in line with the size of the dataset considered (i.e., the larger the dataset, the more efficient the algorithm).

2. Prior work

In recent years, researchers have used statistical analyses (Principal Component Analysis PCA) and/or data mining methods (clustering algorithms) to outline the shape variation of the human body from 3D anthropometric data [1,5,15,17–19,24,26]. These studies were facilitated by Allen et al. [1] who further developed a method called point set registration [8, 9] for the study of 3D shapes of human body parts. In such technique, a uniform polygon mesh called the template is warped over the raw 3D scans of numerous subjects using regularized transformations, therefore enabling shape comparisons on a point-by-point basis. Theoretically, a point i on the corner of the left eye socket should be identically located across all subjects if they share the same registration process.

PCA is a variable-reduction technique, which aims to decrease the large number of variables (i.e., the number of points in the template mesh) into a smaller set of artificial variables called Principal Components (PCs). Measuring the statistical dispersion of the PCs can provide a reasonable understanding of the shape variability of the population. The study of these dispersions has led researchers to the creation of PC-based clusters [17, 24]. However, the inherent characteristics of PCA have made the process of creating these clusters problematic. First, PCA suffers from the all or nothing dilemma, whereas each variation of a PC's value acts on all the points of the mesh model, often in a confusing and unintelligible manner. Second, the number of PCs to consider in the analysis is often based on subjective assessments, resulting in a non-optimal solution. PCA produces as many components as there are points in the template mesh, accounting for all the variance in the sample. However, compromises have to be made, as the purpose of the analysis is to explain as much variance as possible using as few PCs as possible. Third, interpreting and combining the shape variation caused by each selected PC into meaningful clusters have proved to be difficult, especially when three or more components are used. For instance, these limitations caused Meunier et al. [17] to restrict their grouping study to only two PCs, resulting in a statistical model representing only 50% of the sample's total variance.

Clustering algorithms group objects that are "similar" to each other into clusters. Many clustering methods have been proposed in the past, which all have some advantages and drawbacks. The algorithm's selection is generally application-dependent. Connectivity models such as hierarchical clustering perform well for the generation of compact clusters, but can be slow when analysing large datasets ($O(N^3)$). They may also suffer from the so-called single-link effect, where apparent distant clusters end up connected due to a thin line of objects between them. Density models like DBSCAN [12] or OPTICS [3], and centroid models like k-means [16] and k-medoids [14], are faster to solve, but require input parameters that are usually difficult to define efficiently (e.g., *minPts* and ε for DBSCAN, k for k-means). For example, Niu et al. [18] clustered 3D head scans of Chinese soldiers using a k-means algorithm. They set the number of clusters k to seven beforehand but did not provide any detailed analysis that justified this selection.

3. Contributions

In this study, we introduce an algorithm that divides and classifies small to medium size samples of 3D head scans into clusters. Following a modified hierarchical clustering algorithm, distance metrics between pairs of registered head scans are calculated and implemented in a step-by-step process, where clusters are created one after another (instead of simultaneously) in an enhanced manner. Contrary to conventional hierarchical methods, this approach generates a smaller number of clusters while still complying with the same distance metric requirements and classifying a large ratio of subjects. As shown in section 5, a high level of intra-cluster similarity (head shape similarity of the individuals in the same cluster) can still be achieved with this method.

The paper is organized as follows. In section 4, we first present the point set registration method applied in our study and then move to the introduction of the fundamental notions of standard hierarchical clustering algorithms. We then describe in detail the new algorithm. The algorithm is then tested on a database of 3D head scans. In section 5, an evaluation of the algorithm's performance is presented where we compare our results to those obtained using conventional hierarchical clustering methods. Finally, in section 6, we discuss how the clustering requirements described in the introduction are dealt with in the proposed method, and why it could be considered as a better alternative than other clustering methods for the study of 3D head scan data for small to medium size datasets.

4. Materials and methods

4.1. Point set registration and head alignment

A point set registration method is used in our study to process the raw 3D head scans of participants. Since several registration algorithms exist in the literature, we focused our selection on methods that take advantage of the similarity of the shapes being registered (i.e., the head), and the ability to deal with missing data in the target geometry. Some of our 3D scans may indeed contain missing regions that need to be filled in a practical way. This filling is performed by using the shape curvature information encrypted in the template. For example, if a small region around the top of the head of a subject's scan is missing, the algorithm will automatically fill the missing data points by extrapolating the curvature continuity of the template mesh around this area.

We followed the Optimal Step Nonrigid Iterative Closest Point (ICP) algorithm (N-ICP-A) [2] (Fig. 1), which extends ICP methods to non-rigid deformations. The ICP method assumes that every point in the template model corresponds to the closest point to it on the target model. It then aims to minimize the error (distance) between these pairs of points by finding the least square rigid transformation. This process is replicated until an error threshold value is reached. The N-ICP-A works with an additional stiffness term, which can manage the amount of rigid and non-rigid deformation that can be applied at each iteration.

The optimization problem consists of minimizing a cost function $E(X)$ defined by three error terms; $\bar{E}_d$, E_s and E_l:

$$E(X) = \bar{E}_d(X) + \alpha E_s(X) + \beta E_l(X) \tag{4.1}$$

The data error $\overline{E}_d$ is a weighted sum of the squared distances between the transformed template mesh and the target mesh for fixed vertex correspondences. The stiffness error E_s penalises the weighted difference of the transformations of neighbouring vertices. More specifically, this term ensures that similar deformations are applied to triangles located in the same region of the head. The landmark term E_l is added to guide the start of the transformation, especially when the two meshes are too far apart at the beginning of the registration process. α is the stiffness weight, which influences the amount of rigid and non-rigid deformation that can be performed at a given iteration, and β is the landmark weight that dissipates the effect of the landmark term toward the end of the registration algorithm.

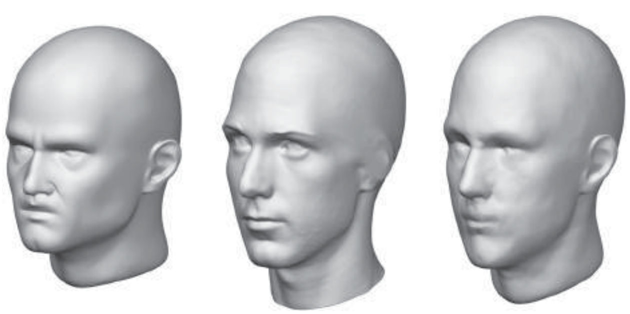

Figure 1. The applied head template mesh, a typical head mesh from the dataset, and the registration result.

The process starts with a high stiffness value, to force nearly rigid transformations, and then release the stiffness gradually as the iterations progress to permit more non-rigid transformations to be applied. For our study, we iterated the process ten times during which the stiffness term was changed in the following way:

$$\textit{for}\ (0 < i \leq 10), \alpha = k_0 e^{\lambda i} \tag{4.2}$$

where i is the iteration number, $k_0 = 5000$, and

$$\lambda = \frac{\ln\left(\frac{k_\infty}{k_0}\right)}{i_{max}} \tag{4.3}$$

with $k_\infty = 15$. Additionally, $\beta = 0.25\alpha$. This optimization scheme was partly based on [13].

Finally, a rigid transformation method was used to align the head scans of our sample after the registration process. This extra step allowed a much greater alignment of the subjects compared to the standard Frankfort plane method. Rigid transformations include rotations and translations, in that order. We defined correspondence vertices between the template and the registered target mesh and applied the Iterative Closest Point (ICP) method [7]. In the algorithm, the reference (template) was kept fixed while the sources (registered targets) were transformed to best match the reference. The estimate combination of the best rotations and translations was defined by a Mean Squared Error (MSE) cost function, which was minimized using a solution based on Singular Value Decomposition (SVD) [4].

For the correspondence, we used the vertices of the 3D mesh lying on the boundary edge of the surface that defined the *proportion of the head that should be under helmet protection* (HPP). This concept was introduced in [10]. This curve position (Fig. 2) is significant for the design of headgear, such as helmets, as it ensures the same position of the main features of the head (i.e.; ears, forehead, and occipital region) for all participants.

The vertices of the mesh located above the blue curve in Fig. 2 were referred to as the Head Covering Points (HCP) and used in the clustering algorithm for the computation of the squared Euclidean distance metric. To our knowledge, this is the first time that clusters are only based on the portion of the head that should be under helmet protection (i.e. face is not included).

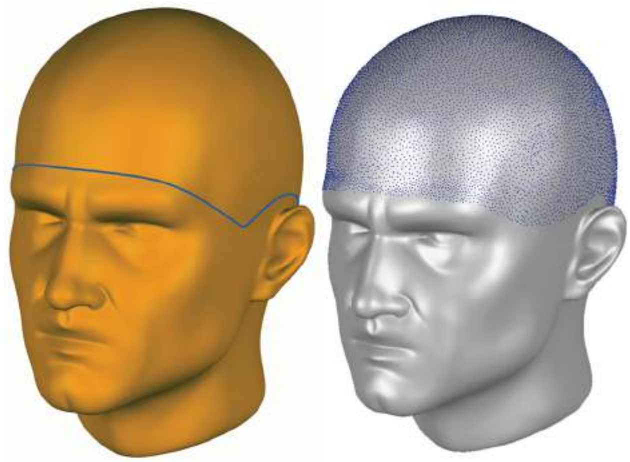

Figure 2. Left: The HPP curve (blue) used to define the vertices in correspondence for the rigid transformation. Right: The Head Covering Points (HCP) used in the clustering algorithm.

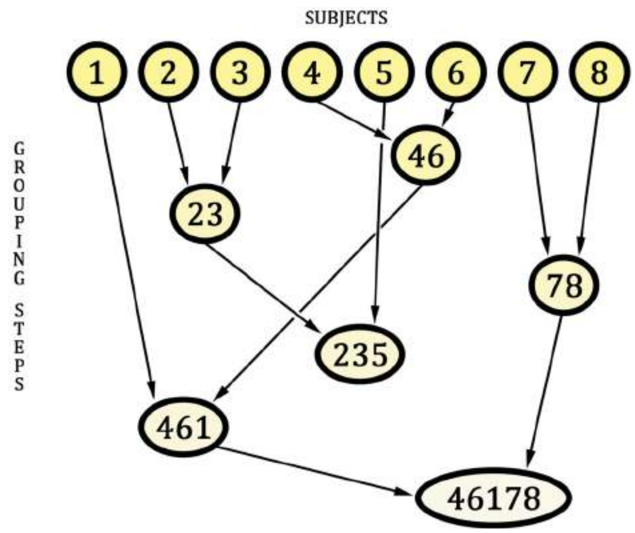

Figure 3. Dendrogram of a classical agglomerative hierarchical clustering.

4.2. Standard hierarchical clustering algorithms

A hierarchical clustering algorithm, also known as linkage clustering, is a method that group objects together into clusters on the basis that close-by objects are more related to each other than objects that are further apart [21]. The common strategy is to use a bottom-up approach, called agglomerative, where N observations start in their own cluster and pairs of clusters are merged together as one moves up the hierarchy. The distances between the objects are computed using a distance metric (e.g., Euclidean distance, squared Euclidean distance, Manhattan distance, Maximum distance). In addition, it is necessary to define a linkage criterion between the clusters since there are multiple objects to compute the distance from when the clusters contain more than one element. The common linkage criteria are:

- *Single-linkage* and *Complete-linkage clustering*, where the distance between clusters equals the distance between the elements (one in each cluster) closest or farthest away from each other.
- *Mean linkage clustering*, where the distance between clusters is equal to the average of all distances between pairs of objects in each cluster.
- *Centroid linkage clustering,* where the distance between clusters is equal to the distance between their respective centroid positions.

The main disadvantage of these methods is the fact that they are not robust against outliers, which can add redundant clusters or cause other clusters to merge (especially for single-linkage clustering).

The algorithm process is typically presented in a Dendrogram (Fig. 3), representing each step of the hierarchical clustering. A threshold value can be set to stop the clustering algorithm before all elements are merged into one cluster. The threshold values generally fall into two categories: (i) a distance criterion, which stops clustering as clusters become too far apart, and (ii) a number criterion, which stops after the specified number of clusters has been reached. In the example in Fig. 3, the algorithm is stopped when eight subjects are grouped into two clusters ({2,3,5} and {4,6,1,7,8}).

4.3. The new clustering algorithm method

Hierarchical clustering methods assume that "close-by objects" are more alike when distance measures between these objects are small. This assumption is particularly true when applied to the comparison of head shapes. Two persons with similar head shape will show small distance values for each pair of points defining their head geometry (i.e. HCP). In our approach, the centroid linkage clustering algorithm was modified in order to sort optimally participants into large, but compactly supported clusters.

In contrast to a conventional hierarchical algorithm, the clusters were generated one after another in the computational process. At each iteration, only one cluster was extracted from the pool of available subjects. The subjects belonging to that cluster were then removed from the dataset before the next iteration. The objective was, therefore, to select the single "best" possible cluster from the data at each iteration. The "best" cluster in our application was one that combined a high level of intra-cluster similarity and a large number of subjects. To achieve this objective, we created multiple clusters candidates at each iteration and used several measures criteria (Section 4.4) to select the "best" cluster.

The algorithm was repeatedly solved until the number of participants classified in one of the clusters had reached a predefined threshold.

The algorithm was developed around four key principles:

1. At each iteration, multiple cluster candidates were computed. One candidate was created for each primary pairwise permutations included in the data (e.g. the merge of subject #4 and subject #6 is a primary pairwise permutation in Fig. 4). For instance, when the algorithm is executed on a dataset of 8 participants, a total of 56 clusters candidates is generated ($\#ClusterCandidates = 2 \times \binom{8}{2} = 56$). However, the odds of computing clusters with the same participants were high. Therefore, only dissimilar clusters candidates were kept for the selection analysis (Section 4.4).
2. The metric employed to determine the next participant to be included in one of the cluster candidate was a squared Euclidean distance, which placed greater dissimilarities on objects that were farther apart. A linkage criterion based on the centroid distance was applied where the HCP coordinates of all participants in a cluster were merged after each step.
3. The distance metric was only calculated for the current cluster candidate and the remaining participants, as the goal was to create only one cluster at the time. In the example below (Fig. 4), after subjects 4 and 6 had been grouped, only six pairwise comparisons (as opposed to 21 for a standard hierarchical clustering) were performed to reveal the next element in the cluster ({4,6} vs 1, 2, 3, 5, 7, 8). Following the same rule, the cluster was built gradually until one of the stopping criteria was reached (Fig. 4: the final cluster is {4,6,1,7,8}).
4. The chosen stopping criterion was the maximum Euclidean distance between any two participants in the cluster at any of the HCPs, after outliers were removed (i.e. distance values outside the whiskers (1.5 times the Interquartile Range)). We used the stopping criterion in two different implementations. In the first one, named *InstaStop*, we stopped the clustering process as soon as the next detected merge of subject had reached the predefined limit. In the second implementation, named *LaterStop*, we discarded such a merge and moved to the next possible subject that passed the criterion. The clustering process was stopped once no more subject could be merged with the current cluster candidate without trespassing the limit.
   In addition, a minimum number of subject in each cluster was required.

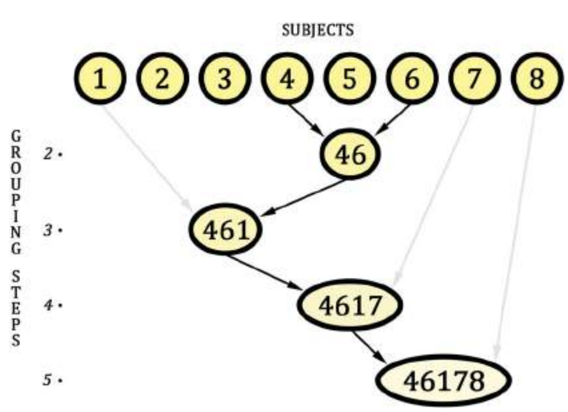

Figure 4. Dendrogram of the algorithm, in which the algorithm starts with permutation {4,6}.

4.4. Best cluster evaluation criteria measures

At each iteration, a combination of four internal quality criteria, namely *a*, *b*, *c*, and *d* was used to optimally select a large cluster with the overall most similar head shapes from the pool of clusters candidates. The combination of these four parameters (i.e. *a* through *d*) provided a broad understanding of the similarity of the head shapes within each cluster. Fig. 5 shows an example of the position dispersion of 30 individuals at one of the HCP (orthographically projected for clarity).

For convention, N is the number of participants in one cluster candidate, n is the number of HCPs, P_{k-j} gives the point coordinates of subjects j within one of the computed clusters at HCP k, the red dot $\overline{P_k}$ is the centroid point of all participants in the cluster at HCP k, and L_{k-j} is the distance between participant j and the cluster's centroid coordinates $\overline{P_k}$ at HCP k.

The four internal quality criteria are defined as follows:

- a is the average mean deviation for each HCP in relation to the cluster's centroid coordinates.

$$a = \frac{1}{Nn} \sum_{k=1}^{n} \sum_{j=i}^{N} L_{k-j} \tag{4.4}$$

- b is the standard deviation of a.
- c is the maximal HCP mean deviation from the cluster's centroid coordinates.

$$c = \max_{k \in [1,n]} \frac{1}{N} \sum_{j=i}^{N} L_{k-j} \tag{4.5}$$

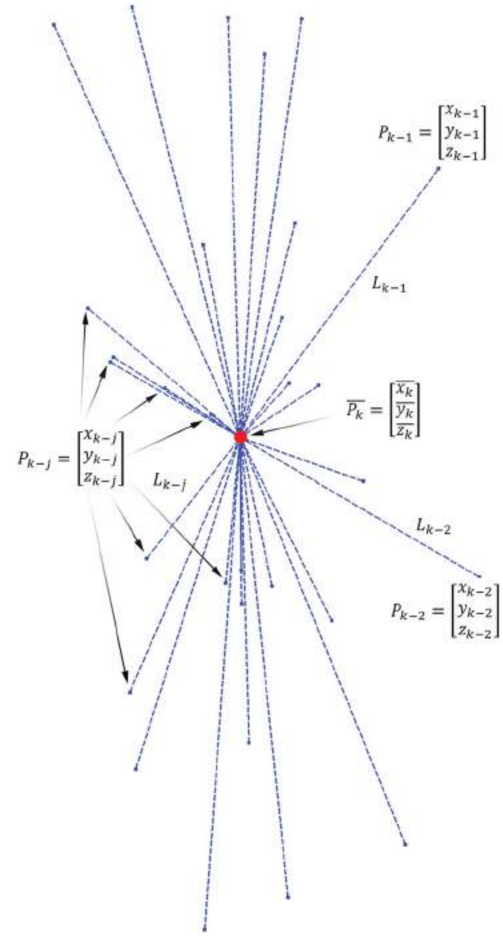

Figure 5. Example of cluster dispersion at one of the Head Covering Point.

- d is the maximal deviation of all L_{k-j} distances.

$$d = \max_{j\in[1,N],k\in[1,n]} L_{k-j} \tag{4.6}$$

Each independent cluster candidate was ranked according to the four parameters. In addition, a weighted average rank was calculated.

$$\begin{aligned} Weighted\ Rank = (& w_a.rank(a) + w_b.rank(b) + w_c.rank(c) \\ & + w_d.rank(d))/(w_a + w_b + w_c + w_d) \end{aligned} \tag{4.7}$$

The weighted rank was then adjusted to take the number of participants in each cluster into consideration, as we sought a compromise between creating large clusters of individuals, and maintaining a high degree of head shape similarity within each of these clusters. To meet these objectives, a negative exponential distribution function with a rate parameter λ was implemented. The Selection Criterion (SC) was defined as

$$SC = \frac{Weighted\ Rank}{\left(e^{\lambda * \frac{Nb\ of\ subjects\ in\ current\ cluster}{Max\ Nb\ of\ subjects\ in\ any\ cluster}}\right) - 1} \tag{4.8}$$

The cluster candidate with the lowest SC was selected as the "best" cluster for the current iteration.

The weights w_a, w_b, w_c and w_d and the rate parameter λ were defined as hyper-parameters in the clustering model. Their values were chosen during the experiment to achieve the largest, but most compactly supported clusters from the clusters candidates at each iteration. We used only 2% of the HCPs (i.e. 260 HCPs) randomly located around the head in this selection process to reduce the computing time.

$$w_a, w_b, w_c, w_d \in [1, 2, 4]\ and\ \lambda \in [1, 5, 10] \tag{4.9}$$

Therefore, a total of 243 ($3^5 = 243$) tests were run beforehand to select the best combinations of hyper-parameters.

4.5. Participants and data collection

The algorithm was applied to the 2014 *3D Anthropometric Database of Australian Cyclists* [20], from which 200 participants were selected to be included in the analysis. Detailed descriptions of the data collection and digitisation processes were presented in [10].

5. Results

5.1. Clusters description

In this example, the algorithm was solved using a distance stopping criterion of 20mm. Furthermore, a cluster had to comprise at least 5% of participants from the initial sample size (i.e. 10 participants). The combination of hyper-parameters that yielded the best clustering results during testing was $w_a = 2, w_b = 1, w_c = 1, w_d = 4$, and $\lambda = 5$.

Table 1. Participants distributions inside the four clusters.

	Cluster 1	Cluster 2	Cluster 3	Cluster 4	Total
Starting sample size (N)	200	92	39	25	200
No. of Participants in the cluster	108	53	14	15	190
Proportion of the full sample (%)	54.0	26.5	7.0	7.5	95.0
Parameter *a* (mm)	4.12	4.23	4.03	4.27	
Parameter *b* (mm)	0.71	0.44	0.61	1.06	
Parameter *c* (mm)	5.61	5.69	5.49	6.39	
Parameter *d* (mm)	11.90	11.37	10.97	11.45	

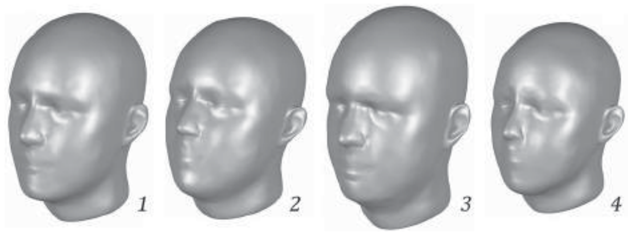

Figure 6. The mean head shape for each of the four computed clusters.

Table 2. Summary statistics of the best cluster selection criteria for cluster 1.

	Mean ± SD	Min	Max
Parameter *a* (mm)	3.65 ± 0.37	2.63	4.42
Parameter *b* (mm)	0.55 ± 0.12	0.28	1.61
Parameter *c* (mm)	5.25 ± 0.74	3.81	10.18
Parameter *d* (mm)	12.58 ± 0.92	10.67	17.98
Cluster size	66.5 ± 24.69	10	113

Using these values on the full dataset and 100% of the HCPs provided (i.e. 13000 HCPs), a total of four clusters were generated by the algorithm, classifying 190 participants from the sample (95.0%). Tab. 1 summarises the results. Fig. 6 shows the mean head shape of the four computed clusters. See [11] for more details on the four created head shapes.

For instance, for cluster No 1, a total of 19900 pairs $\left(\binom{N_s}{2} = 19900 \text{ with } N_s = 200\right)$ were tested twice, with the InstaStop and LaterStop alternatives. 16135 of them were under the 20mm distance threshold value. Amongst the 32270 clusters candidates computed (2×16135), 5091 were dissimilar and were kept for the best cluster selection analysis. Summary statistics of these independent clusters for parameters *a* through *d* and cluster size are listed in Tab. 2.

5.2. Algorithm evaluation

We evaluated our algorithm's performance by comparing the clustering results to four conventional hierarchical methods, specifically the single-linkage, complete-linkage, mean linkage, and centroid linkage algorithms. Similar to the presented study, the distance metric was the squared Euclidean distance, and the stopping criterion was the maximum Euclidean distance between any two participants in the same cluster at any of the HCPs. The distance threshold limit was also set to 20mm. Likewise, the stopping criterion was implemented in the *InstaStop* and *LaterStop* alternatives. Moreover, a cluster had to comprise at least 5% of participants from the sample to be considered as a *final* cluster. The final number of clusters, the number of participants in a cluster, and the mean values of the four key measures are presented in Tab. 3.

6. Discussion

As shown in Tab. 3, the proposed method could classify a high proportion of the participants in the sample into one of the created clusters (95.0%), while still maintaining a small number of partitions (four) compared to the other methods. Some conventional hierarchical algorithms were also able to classify a high proportion of participants (up to 95.5% of the sample), but in order to do so, more clusters were created (up to eight). However, since the parameter values *a* through *d* are slightly higher in our method, we conclude that the resulting clusters are less compact than those obtained from standard hierarchical methods. Nonetheless, the stopping criterion implemented in the process ensured that the maximum distance between any two individuals in a cluster was held under a critical threshold value (20mm is this example) for all clusters.

As the use of 3D anthropometric measurements for product design should not be associated with a significant increase in manufacturing costs, keeping the number of available sizes for a product as small as possible should be of utmost importance when creating 3D sizing systems. Clustering methods of 3D data for product design should, therefore, emphasize on minimizing the number of clusters needed to describe the population, while maximizing the shape resemblance of the

Table 3. Clustering comparison of the 3D head dataset using standards hierarchical methods.

Algorithm	No of clusters	No of participants inside a cluster. Ratio of the sample size.	$\bar{a}(mm)$	$\bar{b}(mm)$	$\bar{c}(mm)$	$\bar{d}(mm)$
New clustering algorithm	4	190 (95.0%)	4.16	0.71	5.80	11.42
Single-linkage *InstaStop*	4	74 (37.0%)	2.75	0.46	4.20	8.77
Single-linkage *LaterStop*	5	176 (88.0%)	3.88	0.61	5.38	11.43
Complete-linkage *InstaStop*	6	75 (37.5%)	2.60	0.39	3.90	9.01
Complete-linkage *LaterStop*	8	191 (95.5%)	3.54	0.54	4.87	10.89
Mean linkage *InstaStop*	6	99 (49.5%)	2.66	0.37	3.83	9.45
Mean linkage *LaterStop*	8	176 (88.0%)	3.34	0.44	4.59	10.56
Centroid linkage *InstaStop*	6	101 (50.5%)	2.82	0.42	3.95	8.98
Centroid linkage *LaterStop*	7	182 (91.0%)	3.43	0.52	4.79	11.02

subjects within each cluster. Taking into account the above, the clustering process would allow the designers to create close-fitted products that could address the current comfort and safety issues encountered in many applications.

However, selecting the *correct* minimum number of clusters for a specific application could be a difficult task. Clustering algorithms such as k-means that require this input parameter could be less suitable than hierarchical methods for the creation of 3D sizing systems.

Unlike multivariate analyses such as Principal Component Analysis (PCA) [17, 24], clustering algorithms can account for most of the sample's head shape variability when creating the size clusters.

The main drawback of hierarchical clustering is the cubic complexity $O(N^3)$ toward the sample size N, which makes it inadequate for large data sets of 3D scans. The overall order of growth of our algorithm's running time was even worse at N^3n for each cluster creation, with n being the number of HCPs. However, the methods could still be competitive for 3D databases containing up to a few hundred subjects. For example, the running time of our algorithm on a standard desktop computer was only six hours for 200 3D head scans and 13000 HCPs, meaning that it would take less than a day to process 1000 subjects defined by 1000 HCPs.

7. Conclusion

In this study, we presented a new method for the clustering of 3D head scans. We based our algorithm on a modified hierarchical method (i.e.; centroid linkage). Multiple pairwise comparisons inside each loop of the hierarchical clustering algorithm were performed, which allowed the creation of several clusters candidates to choose from at each iteration. The selection was based on four parameters (a, b, c, and d) as well as the number of participants contained in each cluster. These measures provided a broad understanding of the head shape similarity within each cluster.

The method was tested on the *3D Anthropometric Database of Australian Cyclists* and compared to other standard hierarchical clustering methods. The new algorithm categorized participants into fewer clusters than standard methods, while still classifying a high ratio of the sample into one of the four computed clusters. However, to quantify that such gains are consistently made, experiments on greater number of data-sets should be performed. The authors intend to apply the new clustering algorithm to other 3D sizing systems of the human body in the future (i.e. for footwear and handwear applications).

Despite the limitations of the proposed method, the study demonstrated that 3D anthropometric data of the head can be summarised and simplified into valuable information for the product designers. These results should encourage ergonomists to use 3D data during the design of head and facial gear.

ORCID

Thierry Ellena http://orcid.org/0000-0003-4917-7125

References

[1] Allen, B.; Curless, B.; Popović, Z.: The space of human body shapes: Reconstruction and parameterization from range scans. in ACM SIGGRAPH 2003 Papers, SIGGRAPH '03. 2003.

[2] Amberg, B.; Romdhani, S.; Vetter, T.: Optimal step nonrigid icp algorithms for surface registration, in Computer Vision and Pattern Recognition, 2007. CVPR'07. IEEE Conference on. 2007. IEEE.

[3] Ankerst, M.; et al.: OPTICS: ordering points to identify the clustering structure, in ACM Sigmod Record. 1999. ACM. https://doi.org/10.1145/304182.304187

[4] Arun, K.S.; Huang, T. S.; Blostein, S. D.: Least-Squares Fitting of Two 3-D Point Sets, *IEEE Transactions on Pattern Analysis and Machine Intelligence, PAMI-9(5)*, 1987, 698–700.

[5] Baek, S.-Y.; Lee, K.: Parametric human body shape modeling framework for human-centered product design, *Computer-Aided Design*, 44(1), 2012, 56–67. https://doi.org/10.1016/j.cad.2010.12.006

[6] Ball, R.: 3-D Design Tools from the SizeChina Project. *Ergonomics in Design: The Quarterly of Human Factors Applications*, 17(3), 2009, 8–13. https://doi.org/10.1518/106480409X12487281219931

[7] Besl, P.J.; McKay, N.D.: A method for registration of 3-D shapes, *IEEE Transactions on Pattern Analysis and Machine Intelligence*, 14(2), 1992, 239–256. https://doi.org/10.1109/34.121791

[8] Blanz, V.; Vetter, T.: A morphable model for the synthesis of 3d faces. 1999.

[9] Blanz, V.; Vetter, T.: Face Recognition Based on Fitting a 3D Morphable Model. 2003.

[10] Ellena, T.; et al.: The Helmet Fit Index – An intelligent tool for fit assessment and design customisation. *Applied Ergonomics*, 55, 2016, 194–207. https://doi.org/10.1016/j.apergo.2016.02.008

[11] Ellena, T.; et al.: 3D digital headform models of Australian cyclists. *Applied Ergonomics*, 59, 2017, Part A, 11–18.

[12] Ester, M.; et al.: A density-based algorithm for discovering clusters in large spatial databases with noise. in Kdd. 1996.

[13] Hasler, N.; et al.: A statistical model of human pose and body shape, *Computer Graphics Forum*, 28(2), 2009, 337–346. https://doi.org/10.1111/j.1467-8659.2009.01373.x

[14] Kaufman, L.; Rousseeuw, P. J.: *Finding groups in data: an introduction to cluster analysis*. Vol. 344. 2009: John Wiley & Sons.

[15] Lacko, D.; et al.: Evaluation of an anthropometric shape model of the human scalp, *Applied Ergonomics*, 48, 2015, 70–85. https://doi.org/10.1016/j.apergo.2014.11.008

[16] Lloyd, S.P.: Least squares quantization in PCM, *IEEE Transactions on Information Theory*, 28(2), 1982, 129–137. https://doi.org/10.1109/TIT.1982.1056489

[17] Meunier, P.; Shu, C.; Xi, P.: Revealing the internal structure of human variability for design purposes, in World Congress on Ergonomics. 2009. NRC.

[18] Niu, J.; Li, Z.; Salvendy, G.: Multi-resolution shape description and clustering of three-dimensional head data. *Ergonomics*, 52(2), 2009, 251–69. https://doi.org/10.1080/00140130802334561

[19] Niu, J.; Li, Z.; Xu, S.: Block Division for 3D Head Shape Clustering, in 2nd International Conference on Digital Human Modeling, ICDHM 2009. Held as Part of HCI International 2009. 2009: San Diego, CA. p. 64–71.

[20] Perret-Ellena, T.; et al.: 3D Anthropometric investigation of Head and Face characteristics of Australian Cyclists. in 7th Asia-Pacific Congress on Sports Technology: Impact of Technology on Sport, APCST. 2015. Barcelona, Spain.

[21] Rokach, L.; Maimon, O.: *Data Mining and Knowledge Discovery Handbook*. 2010: Springer.

[22] Telfer, S.; Woodburn, J.: The use of 3D surface scanning for the measurement and assessment of the human foot, *Journal of Foot and Ankle Research, 2010*. 3(1), 2010, https://doi.org/10.1186/1757-1146-3-19

[23] Yu, Y.; et al.: Digital 3-D headforms representative of chinese workers, *Annals of Occupational Hygiene*, 56(1), 2012, 113–122.

[24] Zhuang, Z.; Benson, S.; Viscusi, D.: Digital 3-D headforms with facial features representative of the current US workforce, *Ergonomics*, 53(5), 2010, 661–71. https://doi.org/10.1080/00140130903581656

[25] Zhuang, Z.; Bradtmiller, B.: Head-and-face anthropometric survey of U.S. respirator users, *J Occup Environ Hyg*, 2(11), 2005, 567–76. https://doi.org/10.1080/15459620500324727

[26] Zhuang, Z.; Viscusi, D.: A new approach to developing digital 3-D headforms, Digital Human Modeling for Design and Engineering Conference and Exhibition, 2008.